EGTRIB Journal
JOURNAL OF
THE EGYPTIAN SOCIETY OF TRIBOLOGY
VOLUME 17, No. 1, January 2020, pp. 13 - 22 **ISSN 2090 - 5882**
(Received November 02. 2019, Accepted in final form December 05. 2019) **www.egtribjournal.com**

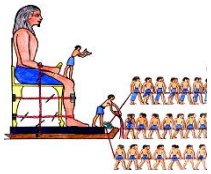

MECHANICAL PROPERTIES OF FRICTION STIR AND GAS TUNGSTEN ARC WELDED AA6061 ALUMINUM ALLOY JOINTS

Mohamed A. S., Mohamed S. S. and Gaafer A. M.

Mechanical Engineering Department, Faculty of Engineering at Shoubra, Benha University, Cairo, Egypt.

ABSTRACT
The present work discusses the mechanical properties of AA6061-O welded joints made by friction stir welding (FSW) and gas tungsten arc welding (GTAW). Al AA6061-O plates of 6 mm thickness using ER4030 filler metal and tungsten electrode (EWth-2) were used in GTAW process. Different arc voltages and welding currents under argon shielding gas were applied. While, friction stir welded (FSW) joints were produced using different tool rotational and welding speeds. Then the welded joints were inspected by X-ray radiography to exclued the defected joints. Micro-hardness, tensile and impact tests were carried out to have specific information on the mechanical properties of the tested welded joints. It was observed that AA6061-O made by (FSW) welded joints had higher mechanical properties than those observed for GTAW.

KEYWORDS
Mechanical Properties, Microstructure, Aluminum alloys, Friction Stir Welding, Gas Tungsten Arc Welding,

INTRODUCTION
The gas tungsten arc welding (GTAW) or tungsten inert gas (TIG) welding is an arc welding process. An inert shielding gas is used in the GTAW process, to protect the welded region from oxidation, where filler is used. GTAW is used to weld alloy steels, aluminum, copper, and magnesium alloys. The quality of the welded joints in GTAW is controlled by workpiece, electrode, filler material, power source type, and the skill of the operator, [1 - 3].

Friction stir welding (FSW) is commonly used marine and aerospace industries, [4]. In FSW, the tool is cylindrical shoulder fitted by threaded pin plunged into the weld line where the shoulder contacts the surface of the workpiece. Then the tool traverses along the weld line. Heat generated due to friction between the shoulder and the surface of the workpiece is sufficient to raise the temperature of the welded region to about 0.8 of the melting temperature. To avoid welding defects that occur from solidification of molten metals, FSW should be performed at lower temperatures. FSW is used for joining high strength aluminum alloys that cannot be welded by fusion welding process.

Fusion welding techniques cannot weld aluminum and its alloys, [5], due to the presence of aluminum oxide film on the surface of the workpiece. Besides, hot cracks and porosity

may occur during the melting and solidification processes. Both of GTAW and FSW techniques are used for welding aluminum alloys. The microstructure and mechanical properties of FSW and GTAW welded joints were discussed, [6 - 11]. Al-4.5Mg-0.26Sc heat-treatable aluminium alloys welded by FSW technique showed higher mechanical properties than those fabricated using TIG, [6]. The welded joints fabricated by FSW and TIG showed reduction in yield strengths by 20% and 50% when compared to the base metal. It was reported that, fatigue strength of FSW of 5052 aluminum welded joints are better than those of TIG welded joints, [7]. FSW had finer grains than the welded joints made by TIG. It is known that fine grain structure can retard the propagation of cracks leading to an increase in fatigue life. It was proved that reported mechanical properties of Al-Mg-Sc welded joints made by FSW were relatively higher than those of TIG welded joints.

The present work discusses the mechanical characteristics and microstructure of AA6061-O aluminum alloy welded joints produced using GTAW (TIG) and FSW welding techniques.

EXPERIMENTAL

AA6061-O (Al-Mg-Si) wrought heat-treatable aluminum alloy was used. The chemical composition of the AA6061 alloy is listed in Table 1, while Table 2 shows the mechanical properties for the AA6061-O alloy in the form of large rolled plates having 6 thickness machined into plates with dimensions of 100 × 250 × 6 mm^3.

Table 1. The chemical composition of the AA6061-O aluminum alloy (wt.-%).

Mg	Si	Fe	Ti	Zn	Cr	Cu	Mn	Al
0.9	0.8	0.13	0.1	0.015	0.35	0.27	0.001	Bal.

Table 2. The mechanical properties of the AA6061-O alloy.

Tensile strength (MPa)	Yield strength (MPa)	Elongation (%)	Hardness (HV)
124	60	25	35

Conventional milling machine was used to carry friction stir welding (FSW), Fig. 1. The tool was made from R18 high speed steel. Different tool rotational and welding speeds were used in FSW. The rotational speeds were 710, 1120 and 1400 rpm while the welding speeds were 63, 80 and 100 mm/min. The angle was 3° while the shoulder plunging depth was 0.2 mm.

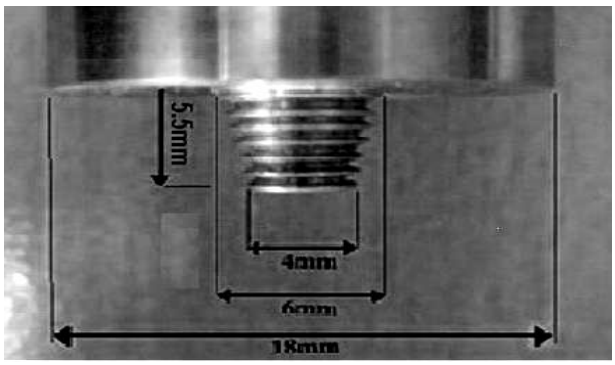

Fig. 1 FSW tool (Dimensions in mm).

The edges of the plates for GTAW process were machined, Fig. 2. The groove was abraded by wire brush, then chemically cleaned by acetone. The GTAW was carried out using a 2.4 mm ER4030 (AlSi5) filler rod with a chemical composition listed in Table 3. The machine used was digitized Fronius Magic Wave 3000. The GTAW was performed using Three values of voltages of 14, 17, and 19 V, and three welding currents of 140, 160 and 175 A were used. An argon was used of 10 l/min flow rate was applied. The Tungsten electrode had 3.2 mm diameter.

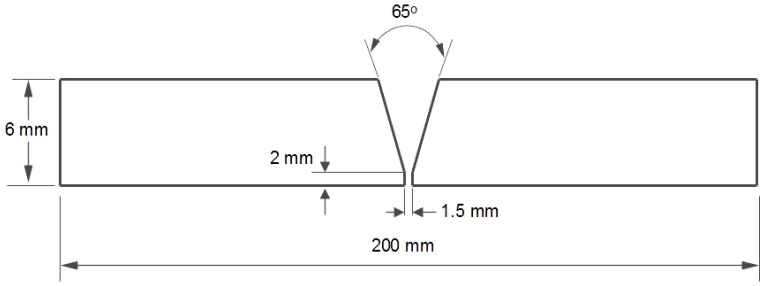

Fig. 2 A schematic illustration of the GTAW joints edge preparation.

Table 3. The chemical composition of the ER 4043 filler (wt. %).

Si	Fe	Cu	Mn	Mg	Cr	Zn	Sn	Al
5.0	0.4	0.1	0.08	0.06	0.25	0.15	0.15	Bal.

The FSW and GTAW joints were examined visually to detect surface defects. The joints were inspected by X-ray radiographic analysis operated at 125 kV, 5 mA for a duration of 1.5 min to detect the pores and discontinuities at weld nugget. The tested samples were cut in a direction perpendicular to the welding direction. Then they were ground and polished using standard metallographic techniques. They were etched by using Keller's reagent. Olympus optical microscope was used to inspect the microstructure, while the grain size measurements were carried out using metallurgical image analyzer.

The measurements of micro-hardness in Vickers were performed on the cross-sections perpendicular to the welding direction. The distribution of the micro-hardness of the welded regions was determined. Tensile tests were carried out, where the test specimens were machined from the welded specimens from the transverse direction with a gauge length of 25 mm and width of 9 mm. The ultimate tensile strength (UTS) of the welded joints was determined. Impact of the tested specimens was carried out by Charpy V-notch tests. The surfaces of the tensile and impact specimens were examined using scanning electron microscope (SEM).

RESULTS AND DISCUSSION

The appearance and X-ray radiography of FSW joint welded using 1400 rpm and 100 mm/min is shown in Fig. 3. They exhibited lateral flash, Fig. 3 a, caused by the outflow of the plastic deformed material that expels material in the form of surface flash. In addition to that, Semi-circular tracks on the surface of the FS welded joints is shown, [12]. No surface cracks were observed. The keyhole defect, at the end of joints, which caused by the welding tool are observed. The joints are free from tunnel defects and cavities, Fig. 3b. It seems that the heat energy produced during FSW was optimum. Based on this observation, it is believed that lower rotational speeds or higher welding velocities may be insufficient to accomplish perfect welding process. For joint welded GTAW using 140 A

and 19 V, the appearance as well as the X-ray radiography are shown in Fig. 4. Where the weld was clean free of welding defects, while Fig. 4b shows that there are no internal defects in GMAW joints.

Fig. 3 Photographs shows (a) general appearance and (b) X-Ray Radiography of joints FS welded using 1400 rpm and 100 mm/min.

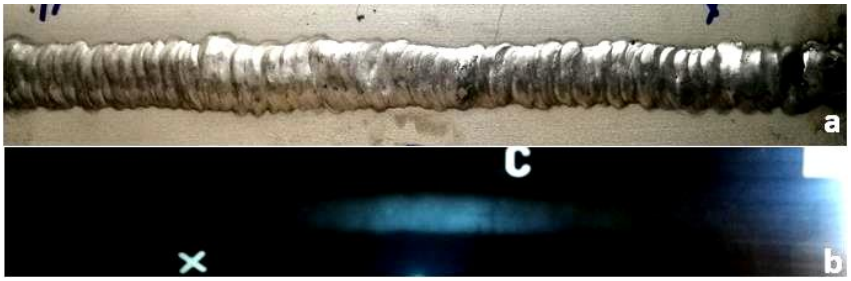

Fig. 4 Photographs shows (a) general appearance and (b) X-Ray Radiography of joints welded by GTAW technique using 140 A and 19 V.

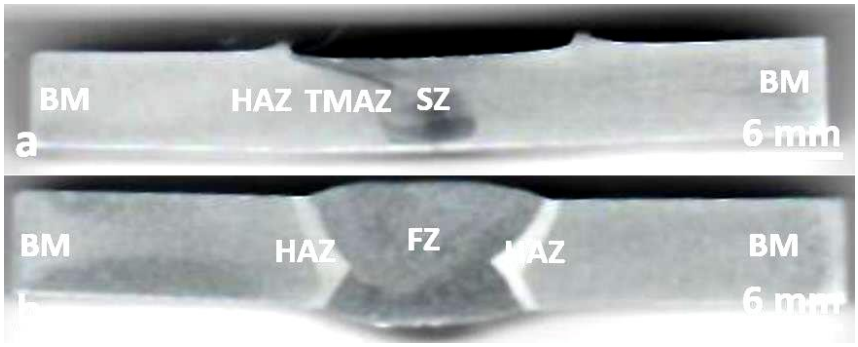

Fig 5 Macrographs of the joints welded using; (a) FSW at 1120 rpm and 100 mm/min; and (b) GTAW at 175 A and 17 V.

The macrographs of the joints welded using FSW and GTAW techniques indicated that the suitable selection of the welding processes parameters, Fig. 5. The different regions of the FS welded joints are the base material, (BM) heat affected zone (HAZ), thermo-mechanically affected zone (TMAZ), and stirred or nugget zone (SZ) are shown in Fig. 5a. Recrystallization process and fusion zone (FZ) with solidification structure were observed in Fig. 5b. The microstructures of base material, stirred zone of a FS welded joint and the fusion zone of a GTAW joint are shown in Fig. 6. Base metal showed large elongated α-Al grains, Fig. 6a. FSW stirred zone showed very fine α-Al grains, while FZ has a microstructure of larger grain size. HAZ grains showed an elongated shape.

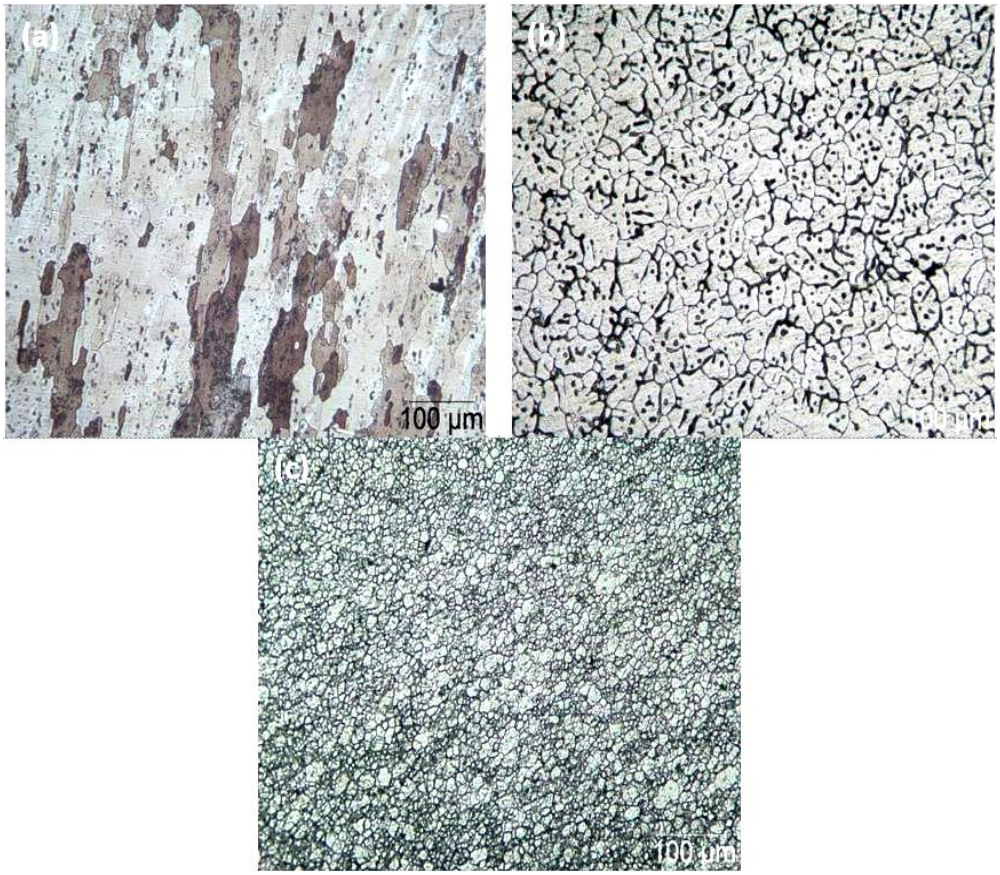

Fig. 6 Optical micrographs for typical microstructures of (a) BM, (b) FZ of GTAW

Variation of the average size, at the center of the welded zone, of the primary α-Al grains with the different FSW and GTAW process parameters is illustrated in Fig. 7. Generally, the FS welded joints exhibited lower grain size at the center of SZ when compared with those joints produced by using GTAW.

In GTAW, the electric arc is used to provide thermal energy to melt the workpiece and the filler materials. After solidification of molten pool metal, a coarsen ingot grain structure is produced. While, in the FSW, the material undergoes intense plastic deformation at elevated temperature (without melting), resulting in the formation of fine grain structure, [9]. For FSW joints, increasing the welding speed and/or tool rotational speed show had a slight influence on the average grain size in the stirred zone. Within the range of the investigated FSW process parameters, the average sizes of the grains at the SZ were found to be vary between 10 to 15 µm. For GTAW, increasing the welding current and/or reducing the welding voltages slightly increase(s) the average size of the primary α-Al grain at the centers of the fusion zones. The minimum and maximum average grain sizes were about 20 and 30 µm, respectively. These values were observed at the center of the fusion zone of joints welded using 140 A and 17 V and 160 A and 14 V, respectively.

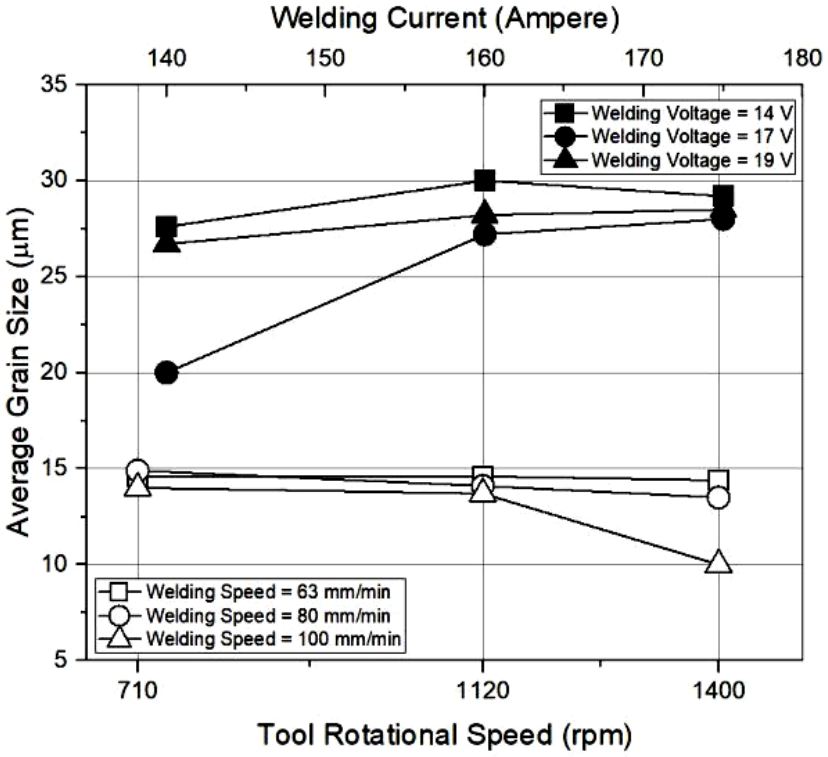

Figure 7. Variation of the average size, at the center of the welded zone, of the primary α-Al grains with the different FSW and GTAW process parameters.

The AA6061-O base metal showed 35 HVN hardness value. Figure 8 shows the micro-hardness profiles of the cross sections of FSW and GTAW joints produced using different process parameters. The micro-hardness of welded regions was higher than the base metal, but the micro-hardness of the FS weld joints was about 15% higher than GTAW joints. The GTAW weld joints showed the highest value of micro-hardness of 68 HVN at weld center. The FS welded joints showed highest value of micro-hardness of about 80 HVN at the weld center. The results revealed that increasing the tool rotational speed and welding velocity slightly increased micro-hardness at FS welded regions. At constant welding speed of 63 mm/min, it was observed that increasing the tool rotational speed from 710 to 1400 rpm had increased the micro-hardness at the center of the SZ from 72 to 80 VHN. The HAZ and TMAZ exhibited higher micro-hardness values compared to the BM.

The increase of the hardness of the FS welded regions when compared with those welded using GTAW may attribute to the finer microstructure in the FS welds. The finer grain structure the better mechanical properties. In case of GTAW welding, very high temperature increases the peak temperature of the molten weld pool causing slow cooling rate, in turn causes relatively coarser grain structure in the fusion zone as observed from the micrographs shown in Fig. 6 b. These microstructures generally offer lower resistance to indentation.

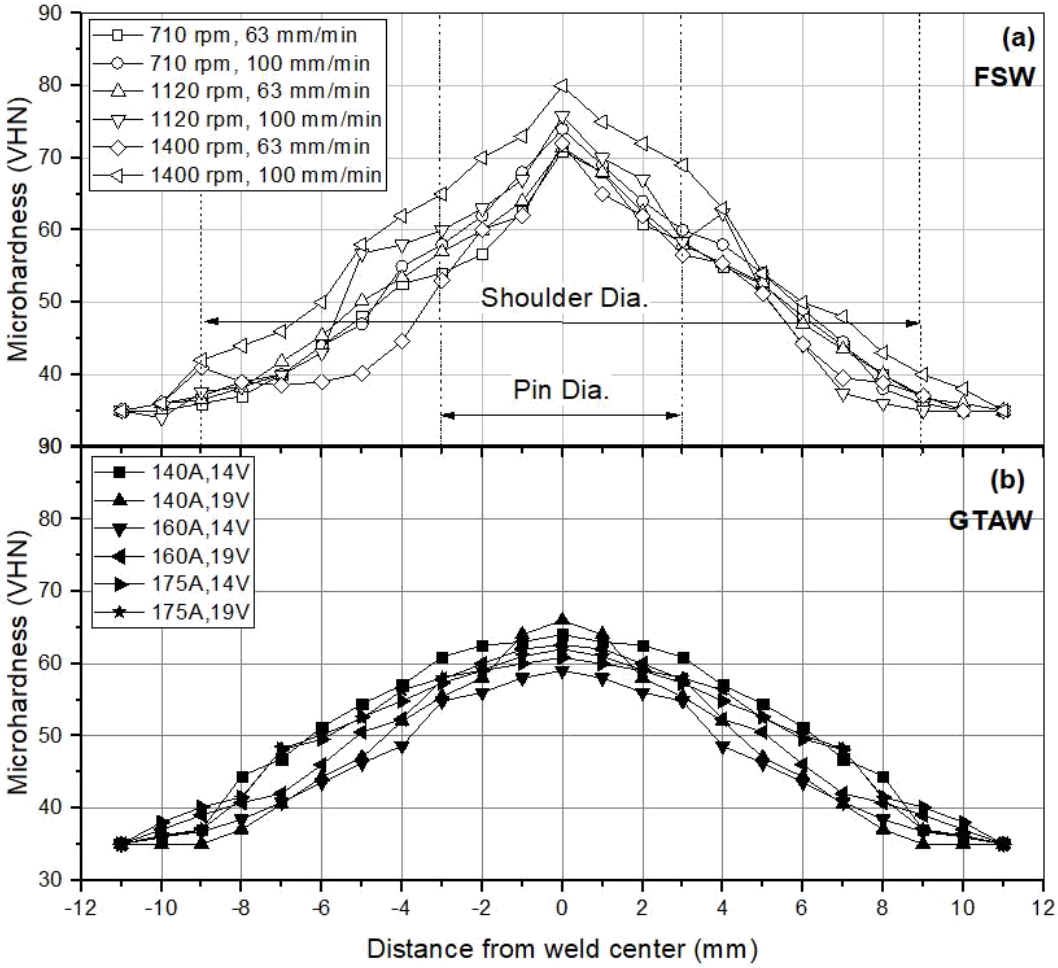

Figure 8. The micro-hardness profiles of the cross-sections of joints welded using: (a) FSW and (b) GTAW at different welding process parameters.

Tables 4 and 5 show the values of tensile strength of FSW and GTAW test specimens respectively. FSW test specimens showed higher tensile strength (145 MPa) than GTAW (128 MPa). Tensile strength of FS welded joints increased as the tool rotational speed and the welding velocity increased. In contradiction to that, increasing welding current form 140 to 175 A decreased the tensile strength of GTAW welded joints.

Table 4. The Tensile strength of FS welded specimens.

Specimen	Tool rotational speed (rpm)	Welding speed (mm/min)	Tensile Strength, UTS (MPa)
1	710	63	126
2		80	120
3		100	134
4	1120	63	129
5		80	133
6		100	137
7	1400	63	130
8		80	139
9		100	145

Table 5. The Tensile strength of GTAW specimens.

Specimen	Current (Ampere)	Voltage (Volts)	Tensile Strength, UTS (MPa)
1	140	14	118
2		17	128
3		19	122
4	160	14	106
5		17	120
6		19	112
7	175	14	110
8		17	100
9		19	115

The cross section of the tensile test specimens are examined by scanning electron microscope (SEM) is shown in Fig. 9. The photomicrographs indicate the ductile fracture mechanism. Coarse dimples were observed at GTAW joints surfaces, Fig. 9 b, while fine dimples for FSW joints, Fig. 9 a.

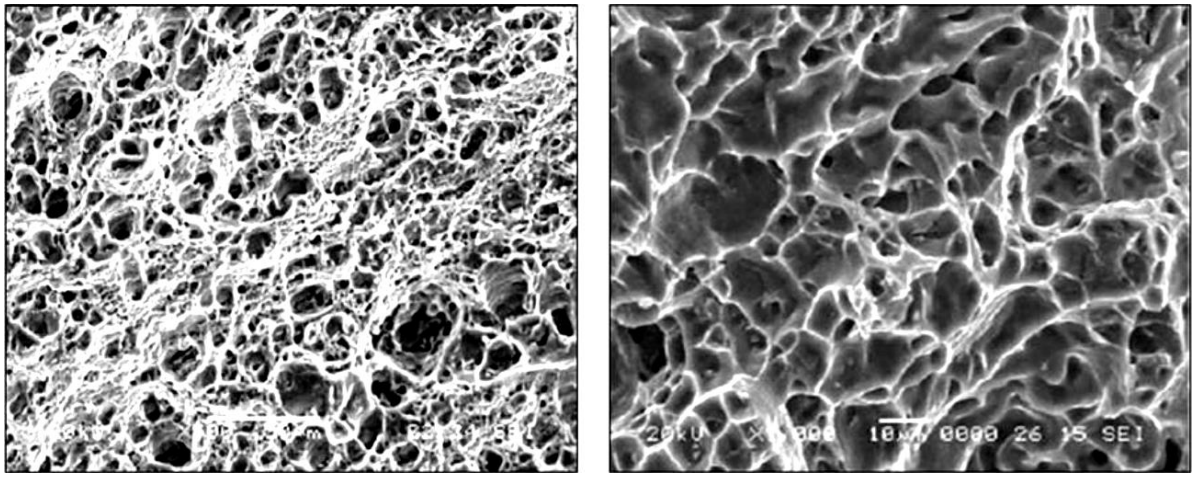

(a) **(b)**

Fig. 9 SEM micrograph of typical fractured surfaces of (a) FSW and (b) GTAW tensile specimens.

The list of the impact strength of FSW and GTAW specimens are shown in Tables 6 and 7, respectively. FSW joints had relatively higher values compared to GTAW joints. The impact strength of the base alloy was about 17 J. The maximum impact strength was about 25 J for specimens FS welded using 710 rpm and 63 mm/min. There was no relation between the impact strength and the tool rotational and welding speeds. The GTAW specimens exhibited significantly lower impact strengths than the base alloy. The maximum impact strength was about 8 J for specimen GTAW using 175A and 19 V.

Table 6. Impact strength of FSW specimens.

Specimen	Tool rotational speed (rpm)	Welding speed (mm/min)	Impact toughness (J)
1	710	63	25
2		80	21
3		100	16
4	1120	63	17
5		80	20
6		100	21
7	1400	63	23
8		80	22
9		100	20

Table 7. Impact strength of FSW specimens.

Specimen	Current (Ampere)	Voltage (volts)	Impact toughness (J)
1	139	14	4
2		17	3
3		19	3
4	160	14	3
5		17	6
6		19	4
7	175	14	5
8		17	3
9		19	8

CONCLUSIONS

1. The FS welded joints showed relatively higher micro-hardness values than GTAW. Micro-hardness slightly increases as the tool rotational speed and welding velocity increase.

2. FSW exhibited higher values of tensile and impact strength than GTAW and AA6061-O base alloy.

3. Tensile strength increased with increasing the tool rotational speed and welding velocity, while impact strength of FSW joints was not influenced by the variation of tool speed or welding velocity.

REFERENCES

1. ASM Handbook, "Welding, Brazing, and Soldering", vol. 6, (1993).

2. Sindo K., "Welding Metallurgy", John Wiley & Sons, 2nd Edition, (2003).

3. Muyiwa O., Paul K. and Jukka M., "Aluminium alloys welding processes: Challenges, joint types and process selection Proc IMechE Part B: J Engineering Manufacture, 227(8), pp. 1129–1137, (2013).
4. Daniela L. and Zhan C., "Friction stir welding: From basics to applications", Woodhead Publishing Limited, (2010).
5. Gene M., "The welding of aluminium and its alloys", Woodhead Publishing Limited, (2002).
6. CabelloMuñoz A., Rückert G., Huneaua B., Sauvage X., Marya S., "Comparison of TIG welded and friction stir welded Al–4.5Mg–0.26Sc alloy", J. of Materials Processing Technology,197(1 - 3), pp. 337 - 343, (2008).
7. Xunhong W., Kuaishe W., Yang S., and Kai H., "Comparison of fatigue property between friction stir and TIG welds", J. of University of Science and Technology Beijing, 15(3), pp. 280 - 284, (2008).
8. Guofu X., Jian Q., Dan X., Ying D., Liying L., and Zhimin Y., "Mechanical Properties and Microstructure of TIG and FSW Joints of a New Al-Mg-Mn-Sc-Zr Alloy", Journal of Materials Engineering and Performance, 25(4), pp. 1249 - 1256, (2016).
9. Xuefeng L., Ying D., Yongyi P., Zhimin Y., and Guofu X., "Microstructure and Properties of TIG/FSW Welded Joints of a New Al-Zn-Mg-Sc-Zr Alloy", Journal of Materials Engineering and Performance, 22, pp. 2723 - 2729, (2013).
10. Morteza Gh., Kazemi M., Sefat M., Aziz A. and Kamran D., "Evaluation of dissimilar joints properties of 5083-H12 and 6061-T6 aluminum alloys produced by tungsten inert gas and friction stir welding", Proc IMechE Part L: J Materials: Design and Applications, 231(3), pp. 297 - 308, (2017).
11. Zhao J., Jiang F., Jian H., Wen K., Jiang L., Che X., "Comparative investigation of tungsten inert gas and friction stir welding characteristics of Al–Mg–Sc alloy plates" Materials and Design, 31, pp. 306 - 311, (2010).
12. Podržaj P., Jerman B., Klobčar D., "Welding Defects At Friction Stir Welding", Metalurgija, 54 (2), pp. 387 - 389, (2015).